IIETA International Information and Engineering Technology Association
Advancing the World of Information and Engineering

Annales de Chimie - Science des Matériaux
Vol. 50, No. 4, August, 2026, pp. 327-336
Journal homepage: http://iieta.org/journals/acsm

# Effect of Chitosan Concentration on the Properties of PEG/PVP Composite Films for Wound Dressing Applications

Zainab Mohammed Sahib*, Asra Ali Hussein

Department of Polymer and Petrochemical Industries, College of Materials Engineering, University of Babylon, Babylon 51002, Iraq

Corresponding Author Email: mat257.zanab.mohammed@student.uobabylon.edu.iq



https://doi.org/10.18280/acsm.500402

**Received:** 2 June 2026
**Revised:** 17 July 2026
**Accepted:** 12 August 2026
**Available online:** 31 August 2026

***Keywords:***
*chitosan, contact angle, composite film, mechanical properties, Polyethylene glycol, Poly(vinylpyrrolidone), solution casting, wound dressing*

**ABSTRACT**

Wound dressings must combine mechanical strength, surface hydrophilicity, and antibacterial activity, which remains a technological challenge. Poly(vinylpyrrolidone) (PVP)/Polyethylene glycol (PEG) composite films containing 0, 8, 10, and 12 wt.% chitosan (CS) were prepared by solution casting and evaluated as candidate wound dressings using Fourier Transform Infrared (FTIR) spectroscopy, Scanning Electron Microscopy (SEM), differential scanning calorimetry (DSC), contact angle measurement, tensile and scratch testing, and antibacterial assays against Staphylococcus aureus and Escherichia coli. FTIR confirmed intermolecular hydrogen bonding between the polymer components, indicating compatibility and miscibility within the blend. SEM showed that increasing CS content improved surface homogeneity and compactness, with the 12 wt.% film exhibiting the most uniform morphology and smallest pore size. DSC revealed that CS incorporation reduced crystallinity and improved polymer compatibility through overlapping thermal transitions. The 12 wt.% film showed the best mechanical performance, with a tensile strength of 11.42 MPa and an average contact angle of 43.56° (±3.51°), confirming adequate surface hydrophilicity. Disc diffusion assays showed no inhibition zones against either bacterial strain, indicating that this method could not confirm antibacterial activity under the tested conditions. These findings suggest that CS incorporation improves the structural, thermal, and mechanical properties of PVP/PEG films, though further antimicrobial functionalization is needed before clinical evaluation.

## 1. INTRODUCTION

The skin acts as the main physical and biological barrier that separates the body from its exterior environment, ensuring that dehydration, physical injury, heat damage, and infections are effectively protected against. Normally, the skin possesses self-healing abilities; however, in the case of both acute and chronic wounds, damage to the structure of the skin makes it impossible for wounds to spontaneously heal [1].

Wound healing involves hemostasis, inflammation, proliferation, and tissue remodeling that must be precisely synchronized to ensure a good outcome. However, among factors that might disrupt the process of wound healing, microbial infections prove to be of major concern by sustaining the pro-inflammatory environment, preventing the growth of keratinocytes and fibroblasts, and inhibiting wound development. In the world, about 300 million individuals suffer from wounds, which are especially susceptible to microbial infections, which make their healing difficult and prolong hospital stays [2-4]. There is a strong need for a dressing method that can aid in healing while minimizing the risks of microbial colonization.

Traditional methods such as gauze, sutures, and adhesives cannot create moisture in the microenvironment, fail to adequately protect the wound from the colonization of additional microbes, and adhere to the surface of the wound bed, leading to pain when removed. Moreover, regular changing of dressings adds to the burden of treatment costs and patient distress, necessitating the development of new wound dressing technology [5, 6].

Hydrogel films composed of biocompatible polymers constitute promising materials for application in advanced wound dressings based on their capability to adsorb wound exudates, create a moist environment for wound healing, and imitate the natural extracellular matrix, facilitating cellular adhesion and proliferation. The mixture of chemically complementary polymers allows for combining mechanical, thermal, and biological properties that cannot be achieved by means of using only one polymer [7-10]. Poly(vinylpyrrolidone) (PVP) is utilized in order to obtain film-forming ability, chemical stability, and application experience of the film-forming system in the field of biomedical science and wound dressing [11, 12]. Polyethylene glycol (PEG), as a plasticizer of the system, decreases the glass transition temperature of the film and increases its flexibility due to the hydrogen-bonding interactions of hydroxyl groups of PEG with carbonyl groups of PVP. Thus, a PVP-PEG interpolymer complex is created [13-15]. Chitosan (CS) is an

active bio-component; it is a partially deacetylated polymer derivative of chitin. CS is characterized by such advantages as hemostatic effect, antimicrobial action, biocompatibility, and biodegradability [16, 17]. Due to its chemical structure, the amino and hydroxyl functional groups of CS molecules may interact with PVP and PEG, which could modify the properties of the composite material.

Despite the detailed investigations devoted to the creation and use of both PVP/PEG-based films and CS-containing wound dressings, previous research mainly focuses on the preparation and performance of these materials. However, it should be noted that there are insufficient data concerning the effect of increasing the CS content on the properties of PVP/PEG/CS composites within the same film-forming system. Moreover, additional research is needed in order to evaluate the effect of a progressive increase in the amount of CS in PVP/PEG/CS films on their mechanical, thermal, surface, and physicochemical properties. Although there is some information about the creation of PVP/PEG/CS composites and intermolecular interactions in these systems, including functional group interactions identified with the help of spectroscopic methods [18, 19], there are insufficient data about concentration-dependent changes of such composites within the specific CS content under investigation. Therefore, the establishment of such dependencies would be useful in order to optimize the compositions of PVP/PEG/CS films for their use as wound dressings. For this reason, in the current study, a systematic investigation of PVP/PEG/CS composite films containing four different concentrations of CS (0%, 8%, 10%, and 12%). The properties of the films were studied using Fourier Transform Infrared (FTIR) spectroscopy, differential scanning calorimetry (DSC), Scanning Electron Microscopy (SEM), contact angle, scratch, tensile, and antibacterial activity tests.

## 2. MATERIALS AND METHODS

### 2.1 Materials

The CS was obtained as white to pale brown colored flakes (Molecular Weight (MW) = 3,800-20,000 g/mol) from HIMEDIA, India. The PEG was obtained as a white wax-like substance (MW = 1,500 g/mol) from Alphachemika, India. The PVP was obtained as a white powder (MW = 40,000 g/mol) from Unilong Industry Co., Ltd., China. Acetic acid (analytical grade) and distilled water were used in this study.

### 2.2 Films formulation

Four films with different amounts of CS and the same solid concentration of 2 g for all formulations were developed. The weight percentages in Table 1 show the composition of solids in each film formulation. CS was added in solution form to the films in amounts of 8, 10, and 12 mL, and the composition of each film was calculated based on a dry-solid basis. The weight percentages were calculated using the formula below:

$$wt.\% = \frac{Mass\ of\ component\ (dry\ basis)}{Total\ dry\ mass\ of\ components} \times 100$$

The total dry weight of the polymeric components was maintained at 2 g for all films.

**Table 1.** Weight percentages of materials used for the preparation of the composite film

| Samples | PVP wt.% | PEG wt.% | CS wt.% |
|---|---|---|---|
| S1 | 55 | 45 | 0 |
| S2 | 51 | 41 | 8 |
| S3 | 50 | 40 | 10 |
| S4 | 49 | 39 | 12 |

Note: Poly(vinylpyrrolidone) (PVP), Polyethylene glycol (PEG), chitosan (CS).

### 2.3 Preparation of PVP/PEG and PVP/PEG/CS composite films

Composite films were prepared through solution casting, where the amounts of the components used are presented in Table 1. Pure PVP/PEG films were prepared by dissolving PEG in distilled water with continuous stirring at 50 ℃. After that, PVP was added gradually while stirring continued. The mixture was stirred for 2 hours, after which it was cast in Petri dishes to be dried under room conditions for 4-5 days. When preparing PVP/PEG/CS films, the CS flakes (2 g) were dissolved in 100 mL of 2% acetic acid for 15 hours at 40 ℃. First, PEG 1500 and PVP K30 were dissolved in distilled water for 2 hours at 50 ℃. Then, the prepared CS solution was added to the solution and stirred for an additional 2 hours at 40 ℃.

After that, the solution was cast in Petri dishes as shown in Figure 1. The composition of each formulation was calculated based on a fixed final total solid content; therefore, the masses of PVP, PEG, and CS were adjusted so that the total mass of the three polymers remained constant at 2 g in all formulations.

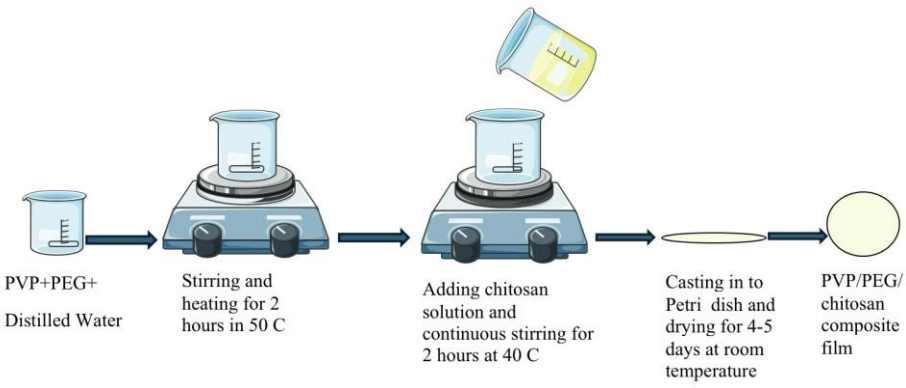


**Figure 1.** Preparation method of Poly(vinylpyrrolidone) (PVP)/Polyethylene glycol (PEG)/chitosan (CS) films

## 3. CHARACTERIZATION METHODS

FTIR spectroscopy was conducted using an IR Affinity-1 Shimadzu spectrophotometer (Japan) in the wavenumber range 4000-500 $cm^{-1}$ to gain information about chemical structure and the presence of functional groups. Thermal characteristics of the obtained films were investigated using DSC (DSC-60 Plus, Shimadzu, Kyoto, Japan). Morphology, homogeneity, porosity, and distribution of the components within the polymeric matrix were visualized with SEM (SEM, FEI Company, Japan). Quantitative analysis of pore size was done with ImageJ software, where nine pores per sample (n = 9) were measured and then the average pore size was calculated. Water contact angle was determined using SL200C Optical Dynamic/Static Interfacial Tensiometer and Contact Angle Meter (KINO Industry Co., Ltd., USA). All the samples were studied under the same testing conditions. Distilled water droplet 5 µl was dispensed on the surface of each film, and the contact angle was recorded after 18 s of water deposition. The software automatically calculated left and right contact angles, and then the average contact angle was determined. Measurements (n = 3) were carried out independently at three locations of the film, and results were expressed as mean ± standard deviation (SD). Tensile characteristics of the films were determined according to the procedure described in the ASTM D882-01 standard by the universal testing machine (TIME Group Inc., China). Samples of 80 mm × 10 mm dimensions were tested at the crosshead speed of 10 mm/min. The thickness of the films was measured at five different positions on each sample using the digital Vernier caliper (resolution of 0.01 mm). The scratch resistance of prepared films was studied using the Automatic Scratch Tester (Model DZ-113). The test was performed using the 1 mm diameter stainless steel sphere as an indenter. The indenter moved along the film surface at a constant scratch speed of 10 mm $s^{-1}$ for 10 mm scratch length with applied loads of 1.5 N and 2.0 N. All the samples were studied under the same testing conditions regarding the geometry of the indenter, scratch speed, scratch length, and loads. After the scratch testing, the scratched surfaces were studied using the digital optical microscope, and appropriate micrographs were taken. The scratch width (mm) was determined perpendicularly to the scratch direction from the micrographs using HiView software for the analysis of images provided by the digital microscope. Antibacterial activity of PEG/PVP/CS composite films was investigated using the disk diffusion method against Staphylococcus aureus (ATCC 29213, Gram-positive) and Escherichia coli (ATCC 25922, Gram-negative). Circular film specimens (diameter 10 mm) were aseptically deposited on Mueller Hinton Agar (MHA) plates inoculated with bacteria suspension at 0.5 McFarland turbidity (approximately $1 \times 10^8$ CFU/mL). Plates were inoculated uniformly in three directions with a sterile cotton swab. Then the plates were incubated upside-down at 37 °C for 18-24 h, and the inhibition zone was measured around each specimen.

## 4. RESULTS AND DISCUSSION

### 4.1 FTIR spectroscopy results

FTIR spectra analysis confirms the presence of characteristic functional groups of PVP, PEG, and CS in the prepared films, as shown in Figure 2. The broad band from 3200 to 3500 $cm^{-1}$ is due to overlapping O-H and N-H vibrations. The broadening of this band in the films containing CS can be due to the presence of hydroxyl groups in both PEG and CS, amino groups of CS, and possible hydrogen bonding interaction among the blend components [20, 21]. The band at 2885 $cm^{-1}$ is due to aliphatic C-H stretching vibration ($–CH_2$) vibrations of PEG and the polymer backbone [22]. The characteristic carbonyl (C = O) stretching vibration of the pyrrolidone ring of PVP shows up at about 1651.07 $cm^{-1}$ in the PVP/PEG film and is shifted to 1658.78 $cm^{-1}$ after inclusion of CS. This small peak shift suggests that there might be some interactions between the carbonyl group of PVP and the hydroxyl and amino groups of CS, possibly through hydrogen bonding [23, 24]. The band at 1465 $cm^{-1}$ is attributed to bending vibrations of $CH_2$ belonging to PEG and other aliphatic polymer chains [23]. Another band at 1350 $cm^{-1}$ is due to C-N stretching vibrations belonging to CS and the pyrrolidone ring of PVP [25]. The band at about 1103 $cm^{-1}$ is due to stretching vibrations of C-O-C of the ether groups of PEG and glycosidic linkages of CS. Bands at 948 $cm^{-1}$ and 840 $cm^{-1}$ correspond to skeletal vibrations of PEG, $CH_2$ rocking, and crystalline phase vibrations of PEG chains. Thus, almost all of the characteristic bands appear at similar wavenumbers except for the small peak shift for the C = O band after CS inclusion. These results suggest that there is good compatibility of polymer components without the creation of any new chemical bonds. Good compatibility is essential for wound dressing material since it allows forming uniform films with good structural stability without affecting the functional groups of the polymers.

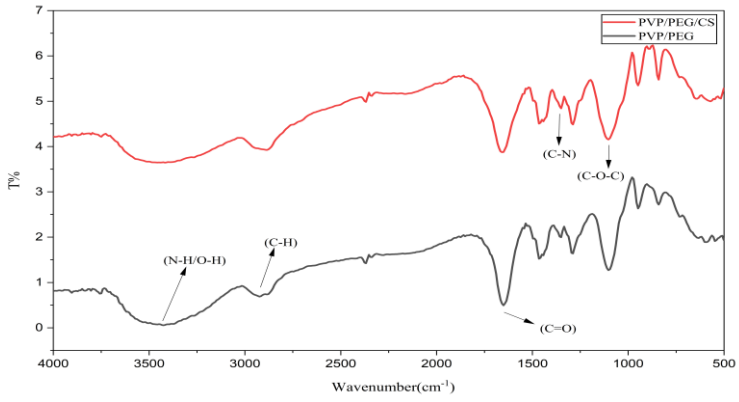


**Figure 2.** FTIR spectroscopy test results of Poly(vinylpyrrolidone) (PVP)/Polyethylene glycol (PEG) (black) & PVP/PEG/chitosan (CS) (red) composite films

### 4.2 Differential scanning calorimetry analysis

Thermal properties of the polymeric systems were estimated using DSC thermograms shown in Figure 3. In the case of the PVP/PEG polymeric system, there is an endothermic peak seen at ~44 °C that corresponds to the melting temperature Tm of the PEG-containing phase. This thermal temperature is characteristic of the melting behavior of PEG, and it is consistent with previous reports of PEG/PVP based polymer systems. Another thermal peak in the PVP/PEG system is seen at 126 °C and is related to relaxation or partial molecular rearrangement due to the interaction between polymer chains. Also, another transition near 148 °C is connected to partial molecular rearrangement of the amorphous polymer framework [26-28].

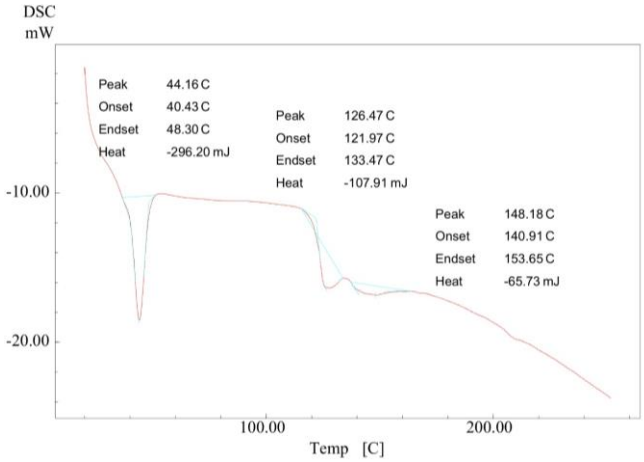


(a) Differential scanning calorimetry (DSC) analysis for S1

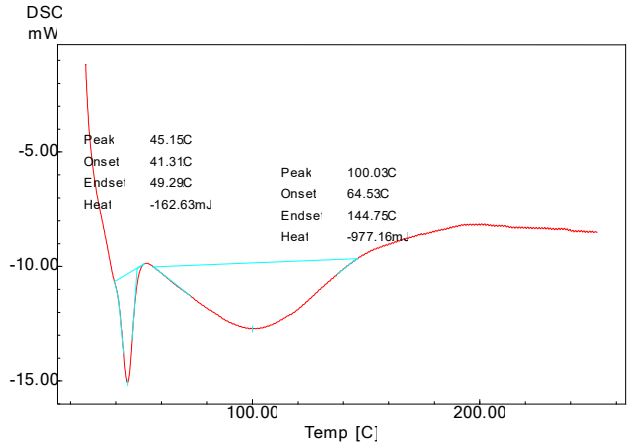


(b) Differential scanning calorimetry (DSC) analysis for S4

**Figure 3.** Differential scanning calorimetry (DSC) thermograms of (a) Poly(vinylpyrrolidone) (PVP)/Polyethylene glycol (PEG) and (b) PVP/PEG/12% chitosan (CS)

The addition of CS leads to considerable changes in the thermal characteristics of the investigated polymer systems. First of all, there is a distinct endothermic peak around 100 °C, and this fact indicates the existence of strong intermolecular interactions. The intermolecular interactions in this system may be explained by hydrogen bond formation between the carbonyl (C = O) groups of PVP, hydroxyl (–OH) groups of PEG, and amino ($–NH_2$) groups of CS. Moreover, changes in the peak width and peak shift may show good compatibility between polymer constituents. The absence or merging of some peaks may indicate low crystallinity of the polymer matrix due to the plasticization effect of PEG and CS intermolecular bonds [29].

### 4.3 Scanning Electron Microscopy results

The effect of CS content on the morphological properties of the PEG/PVP composite films was assessed using SEM. Three representative samples of the film with different concentrations of CS were analyzed using the SEM technique: (i) pure PEG/PVP (0 wt.% CS), (ii) PEG/PVP with 8 wt.% CS, and (iii) PEG/PVP with 12 wt.% CS. As shown in Figure 4 (a, b), the pure PEG/PVP film had a rough surface with plenty of pores and voids. The quantitative analysis of the images (n = 9 for each sample) gave a range of pore sizes from 6.68 to 19.78 µm, with an average value of 14.51 ± 4.48 µm.

In the case of the film with 8 wt.% CS Figure 4(c, d) the film surface became more homogeneous, and pores had a more even distribution in contrast to the pure PEG/PVP. The pore size decreased substantially to 3.88-5.83 µm, with an average size of 4.70 ± 0.73 µm. This means that CS inclusion affects the inner structure of the polymer film, leading to the formation of a finer and more homogeneously distributed porous structure.

Adding CS up to 12 wt.% Figure 4(e, f) resulted in the formation of a film with a more compact structure. The pore size was reduced again to 0.74-3.61 µm with an average value of 1.88 ± 1.02 µm. Overall, the results obtained by SEM and pore size analysis show the tendency of the pore size reduction with the increase of CS concentration due to the formation of a denser polymer network because of CS-PVP/PEG interactions [30].

### 4.4 Water contact angle measurement

The wetting ability of the fabricated PEG/PVP/CS composite films was studied by using the static water contact angle test, and the data obtained are given in Table 2 and Figure 5. The bare PEG/PVP matrix (Sample 1) had the lowest value of the water contact angle, equal to 23.72° ± 0.66°, and hence the highest degree of hydrophilicity compared to other samples. Such behavior is related to the presence of hydrophilic polymers, PVP and PEG. Indeed, hydrogen bonds can be formed between the carbonyl (C = O) groups of PVP and the hydroxyl (–OH) ends of PEG and water molecules.

The incorporation of CS results in an increase in the water contact angle from 32.10° ± 2.27° for Sample 2 (8 wt.% CS) to 36.44° ± 1.08° for Sample 3 (10 wt.% CS) and to 43.67° ± 3.56 ° for Sample 4 (12 wt.% CS). However, the value of the contact angle, despite being high, remains below 90°, meaning that all the films are hydrophilic. In other words, hydrophilicity decreases due to the partial hindrance of the hydrogen bonds between the surface of the polymer film and water molecules since the latter interact with the CS.

The FTIR spectroscopy confirms this hypothesis, showing that hydrogen bonds are formed between the amine ($–NH_2$) and hydroxyl (–OH) groups of CS and the carbonyl groups of PVP and the hydroxyl ends of PEG. The higher CS content leads to an increase in the number of these hydrogen bonds; consequently, the number of the surface groups involved in the interactions with the water molecules decreases. These results agree with those found for PVP/CS blend films when the increase in CS content shifts the balance of the surface free energies, leading to a decrease in wettability compared to the pure PVP matrix. It should be noted that hydrophilic films with

CS usually have water contact angles below 90°, which is an important property for the wound dressing material due to the possibility of appropriate exudate adsorption in the moist wound healing environment.

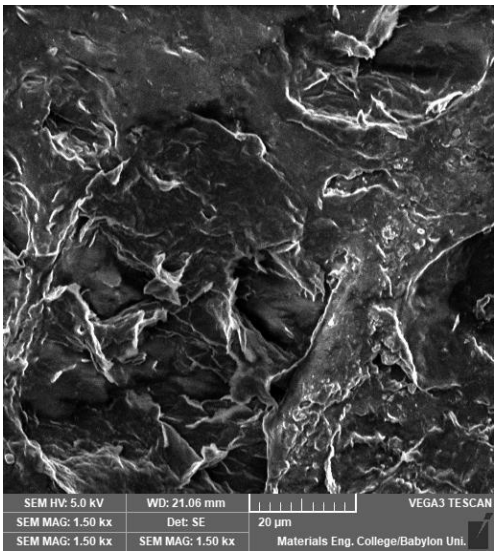


(a) SEM result for S1at 20 µm

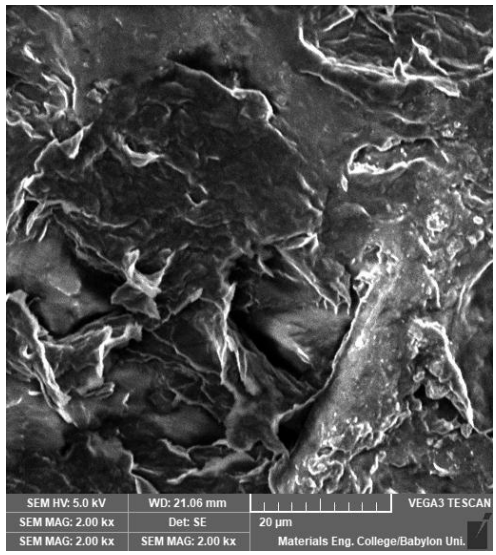


(b) SEM result for S1 at 20 µm

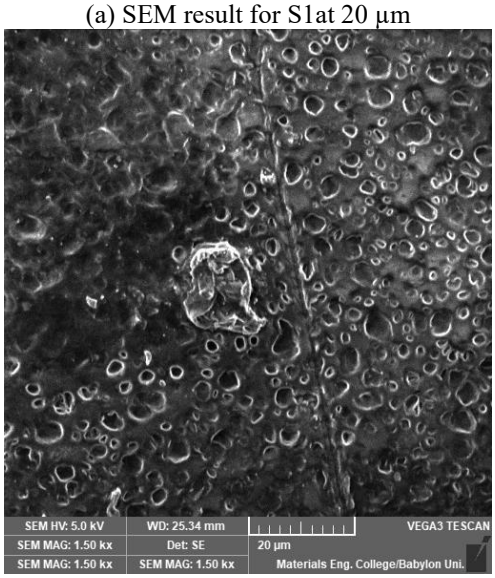


(c) SEM result for S2 at 20 µm

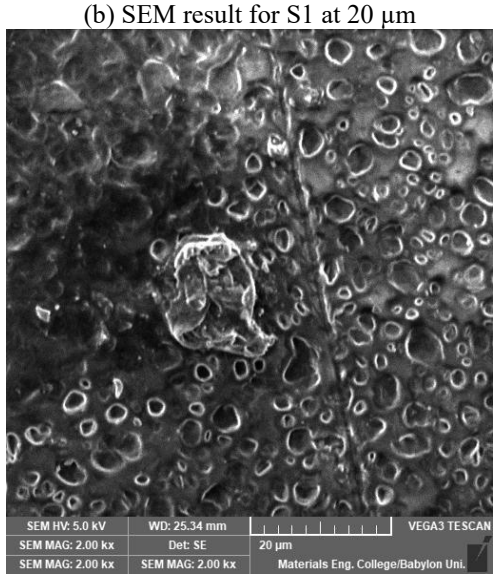


(d) SEM result for S2 at 20 µm

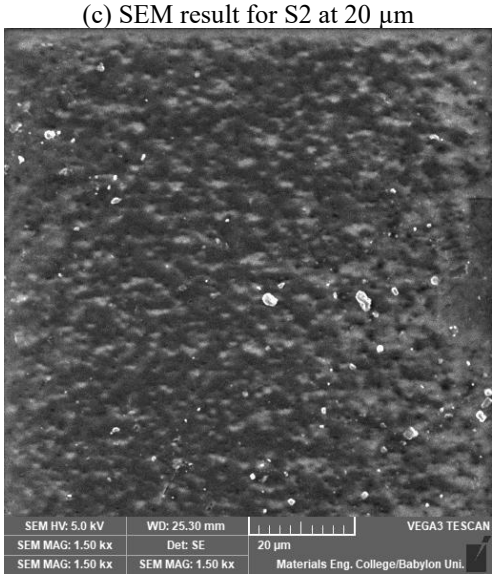


(e) SEM result for S4 at 20 µm

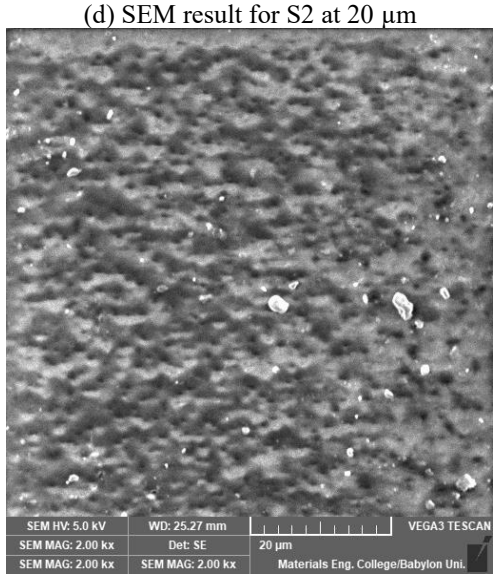


(f) SEM result for S4 at 20 µm

**Figure 4.** Scanning Electron Microscopy (SEM) micrographs of (a, b) Poly(vinylpyrrolidone) (PVP)/Polyethylene glycol (PEG), (c, d) PVP/PEG/8 wt.% chitosan (CS), and (e, f) PVP/PEG/12 wt.% CS films at magnifications of 1.50 kx and 2.00 kx, respectively

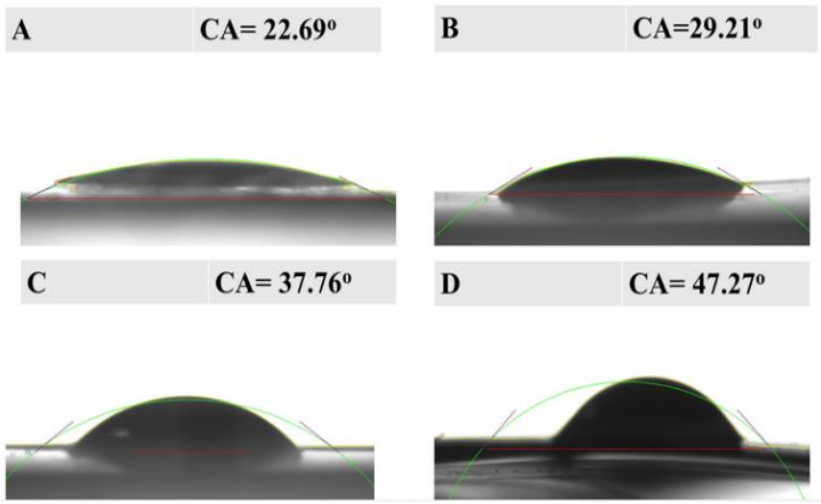


**Figure 5.** Representative contact angle images of the prepared polymer films: (A) sample 1, (B) sample 2, (C) sample 3, (D) sample 4 after 18 s

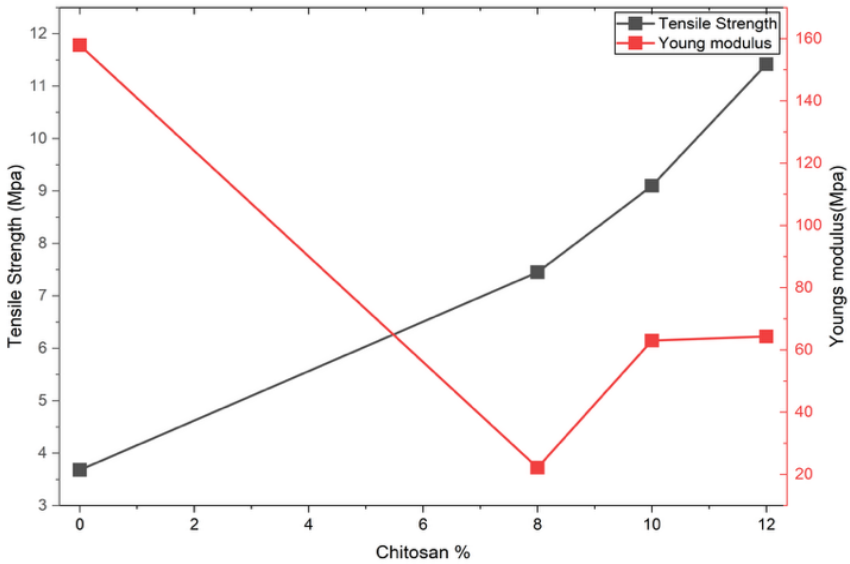


**Figure 6.** Tensile strength (MPa) and Young's modulus (MPa) of Poly(vinylpyrrolidone) (PVP)/Polyethylene glycol (PEG)/CS films as a function of chitosan (CS) content (wt.%)

Such a combination of the properties is beneficial for wound-dressing applications because of improved exudate management [31, 32].

**Table 2.** Contact angle results for composite films

| Samples | Contact Angle (°) Mean ± SD |
|---|---|
| S1 | 23.72 ± 0.66 |
| S2 | 32.10 ± 2.27 |
| S3 | 36.44 ± 1.08 |
| S4 | 43.67 ± 3.56 |

Note: Standard deviation (SD).

### 4.5 Tensile strength

Tensile strength and other mechanical properties of films manufactured using PEG/PVP composites significantly depended on the amount of CS added to the film structure Figure 6. Thus, the control sample (Sample 1) had a rather low tensile strength, which was 3.68 MPa and could be explained by flexible molecular chains of the film. Addition of CS to the film increased the tensile strength, which ranged between 7.45 MPa (Sample 2) and 11.42 MPa (Sample 4). These values indicate positive changes caused by the formation of stable hydrogen bonds between –OH and C = O groups of PEG/PVP and $–NH_2$ and OH groups of CS (23). As for Young's modulus, its values were relatively high (157.9 MPa) in the case of the control sample and decreased dramatically (22.2 MPa for Sample 2). With further increase in CS content, Young's modulus increased (63.0 MPa for Sample 3; 64.3 MPa for Sample 4) due to higher interactions between molecules [33].

### 4.6 Scratch resistance

The scratch width in films was determined for the applied loads of 1.5 N and 2 N Figure 7. As can be seen from the results, the ability of films to resist scratching largely depends on the composition of the composites.

Sample 1 was characterized by the weakest resistance to scratching, with the scratch width showing a considerable increase from 0.885 mm at 1.5 N to 1.281 mm at 2 N, which is related to a large degree of plastic deformation of the film surface subjected to the higher load. Sample 2 had the least

dependence of the scratch width on the load, with the width value practically unchanged at 0.559 mm at 1.5 N and 0.552 mm at 2 N, which is indicative of high structural stability and resistance to deformation induced by load application. Sample 3 had an intermediate scratch resistance, with the width increasing from 0.430 mm 1.5 N to 0.556 mm 2 N. Sample 4 showed the highest scratch hardness with the scratch widths being the smallest 0.389 mm at 1.5 N and 0.549 mm 2 N among all samples. Though, its advantage over Samples 2 and 3 decreased sharply when using the higher load (the values being close-0.549-0.556 mm) [34, 26].

### 4.7 Antibacterial activity

The antimicrobial activity against Gram-positive Staphylococcus aureus and Gram-negative Escherichia coli was tested using the disc diffusion test after 18-24 h incubation. According to Figure 8, there were no observable inhibition zones of both binary and ternary composite films, which suggests that diffusion-based antimicrobial activity did not occur under the applied experimental conditions. Such results can be attributed to poor diffusion of CS from the polymer matrix into the agar medium owing to its poor solubility at neutral pH. Furthermore, interaction between CS and the PEG/PVP polymer matrix reduces diffusion of amino groups to the surrounding medium, which decreases diffusion-based antimicrobial activity [18, 19]. In this work, only the disc diffusion test was conducted; thus, no conclusion can be made about the contact-based antimicrobial activity on the film surface. Special experiments are required in order to test such a property of composite films.

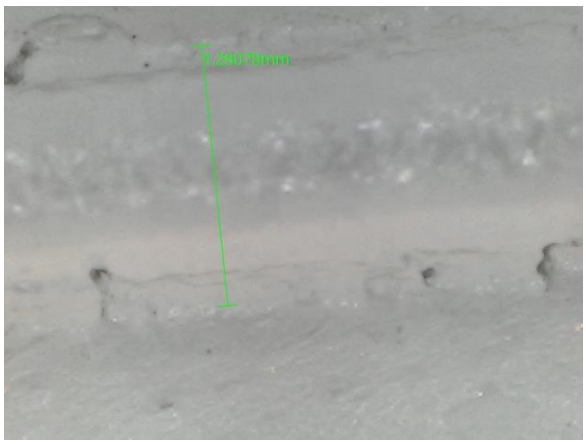

(a) Scratch width of sample 1 at 1.5 N

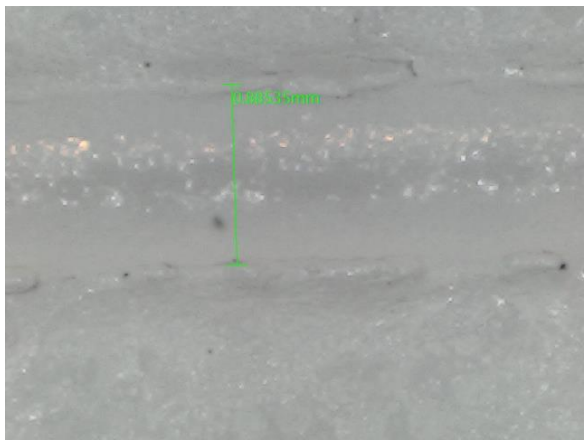

(b) Scratch width of sample 1 at 2 N

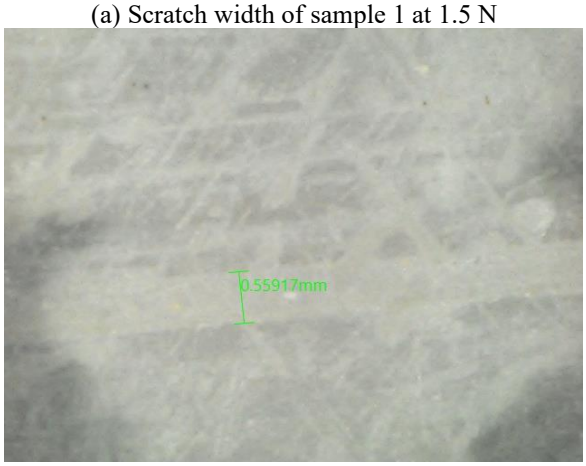


(c) Scratch width of sample 2 at 1.5 N

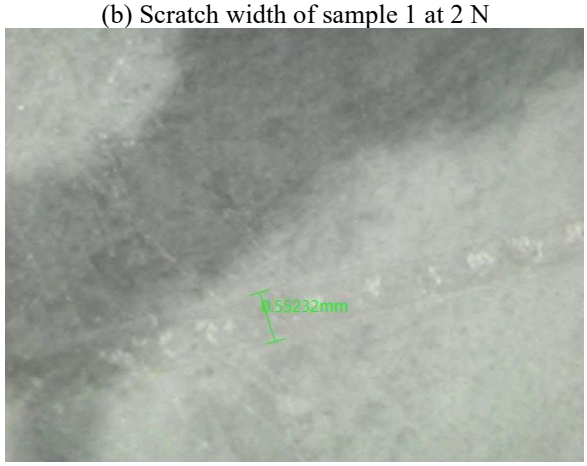


(d) Scratch width of sample 2 at 2 N

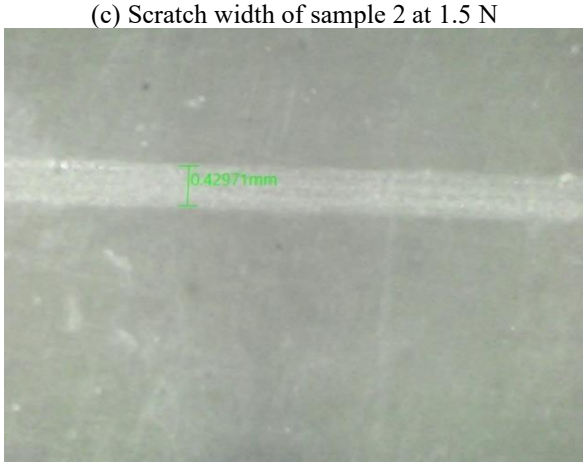


(e) Scratch width of sample 3 at 1.5 N

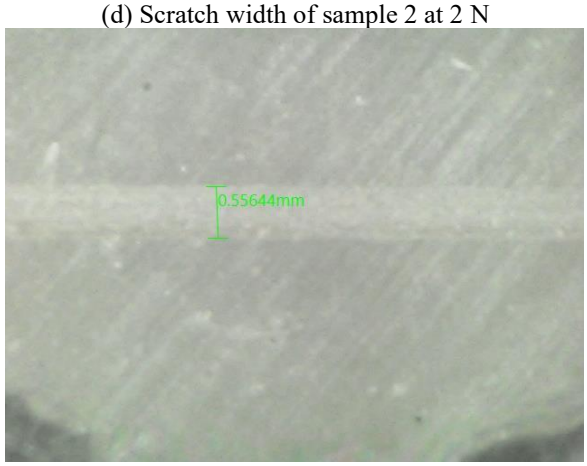


(f) Scratch width of sample 3 at 2 N

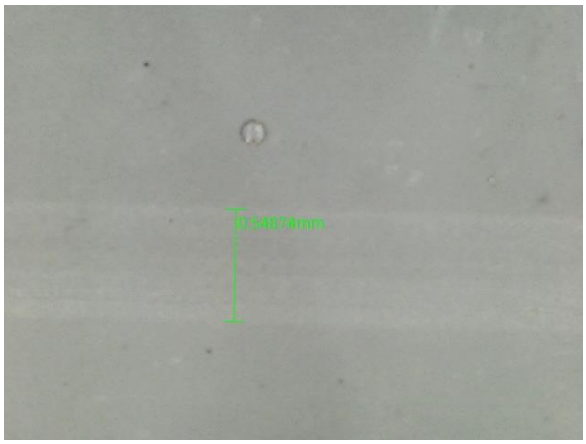

(g) Scratch width of sample 4 at 1.5 N

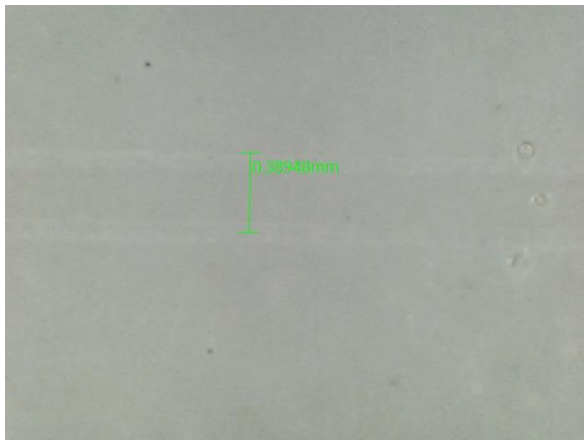

(h) Scratch width of sample 4 at 2 N

**Figure 7.** Optical images showing the scratch width of Polyethylene glycol (PEG)/Poly(vinylpyrrolidone) (PVP)/chitosan (CS) composite films containing different CS concentrations: (a, b) 0 wt.%, (c, d) 8 wt.%, (e, f) 10 wt.%, and (g, h) 12 wt.%

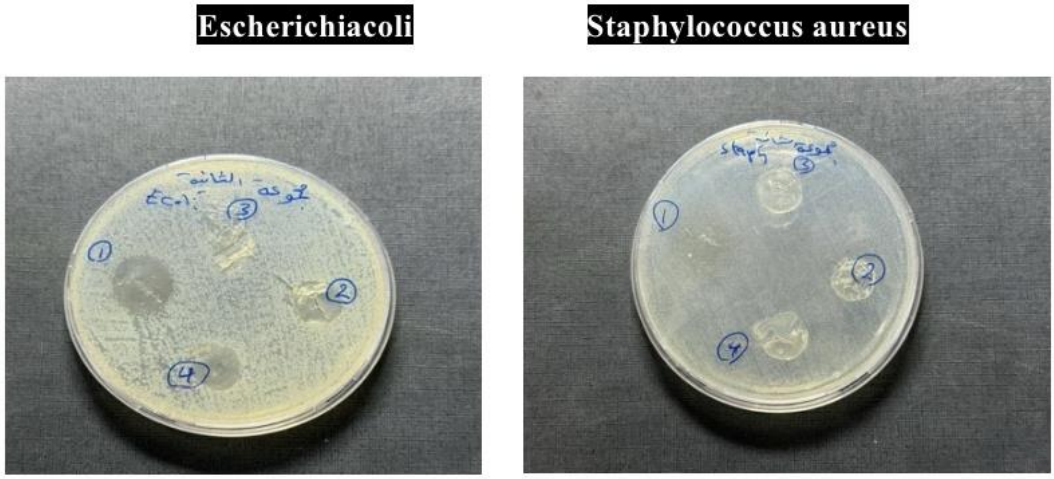


**Figure 8.** Antibacterial activity of Polyethylene glycol (PEG)/Poly(vinylpyrrolidone) (PVP) and PEG/PVP/chitosan (CS) composite films (8 wt.%, 10 wt.%, and 12wt.%) against Escherichia coli (Gram-negative) and Staphylococcus aureus (Gram-positive) using the disc diffusion method

## 5. CONCLUSION

The inclusion of CS in the PVP/PEG composite films has led to obvious, concentration-related improvements in the compatibility of the structural characteristics, surface morphology, thermodynamic stability, and mechanical strength, where the 12 wt.% CS formulation has shown the best combination of these parameters. Such a result proves the idea that CS not only integrates with the PVP/PEG matrix but is engaged in hydrogen bonds, which causes a reconstruction of the film's structure, reducing pore size and improving mechanical properties at once. As a practical result of such research, one can state that the CS concentration can be used as a single tuning parameter that will give the possibility of tuning the film properties according to the needs in mechanical and morphological properties of the wound dressing rather than including several different components for separate properties of the dressing.

It is important to note that this study is limited by its nature. Antibacterial activity was checked using only the disc diffusion method, which allows checking the presence of diffusion-mediated activity and does not allow proving or disproving the ability of the tested substance to act on bacteria in contact mode. The absence of inhibition zones means the limitations of the method rather than the absence of the activity of the substance. The next step in future research should include a contact-inhibition assay in order to check the antibacterial mechanism, which is proposed due to the structure of CS. In vitro cytotoxicity tests, drug-loading, and in vivo wound healing evaluation are needed.

## REFERENCES

[1] Rezvani Ghomi, E., Khalili, S., Nouri Khorasani, S. Esmaeely Neisiany, R., Ramakrishna, S. (2019). Wound dressings: Current advances and future directions. Journal of Applied Polymer Science, 136(27): 47738. https://doi.org/10.1002/app.47738

[2] Simões, D., Miguel, S.P., Ribeiro, M.P., Coutinho, P., Mendonça, A.G., Correia, I.J. (2018). Recent advances on antimicrobial wound dressing: A review. European Journal of Pharmaceutics and Biopharmaceutics, 127: 130-141. https://doi.org/10.1016/j.ejpb.2018.02.022

[3] Liang, Y.P., He, J.H., Guo, B.L. (2021). Functional hydrogels as wound dressing to enhance wound healing.

ACS Nano, 15(8): 12687-12722. https://doi.org/10.1021/acsnano.1c04206
[4] Masoud, A.R., Velisdeh, Z.J., Bappy, M.J.P., Pandey, G., Saberian, E., Mills, D.K. (2025). Cellulose-based nanofibers in wound dressing. Biomimetics, 10(6): 344. https://doi.org/10.3390/biomimetics10060344
[5] Paula, C.T.B., Madeira, A.B., Pereira, P. (2022). ROS-degradable PEG-based wound dressing films with drug release and antibacterial properties. European Polymer Journal, 177: 111447. https://doi.org/10.1016/j.eurpolymj.2022.111447
[6] Liu, S.D., Li, D.S., Wang, Y., Zhou, G.Q., Ge, K., Jiang, L. (2023). Adhesive, antibacterial and double crosslinked carboxylated polyvinyl alcohol/chitosan hydrogel to enhance dynamic skin wound healing. International Journal of Biological Macromolecules, 228: 744-753. https://doi.org/10.1016/j.ijbiomac.2022.12.169
[7] Lutolf, M.P. (2009). Spotlight on hydrogels. Nature Materials, 8(6): 451-453. https://doi.org/10.1038/nmat2458
[8] Zhong, Y.J., Xiao, H.N., Seidi, F., Jin, Y.C. (2020). Natural polymer-based antimicrobial hydrogels without synthetic antibiotics as wound dressings. Biomacromolecules, 21(8): 2983-3006. https://doi.org/10.1021/acs.biomac.0c00760
[9] Zhang, M., Li, X.H., Gong, Y.D., Zhao, N.M., Zhang, X.F. (2002). Properties and biocompatibility of chitosan films modified by blending with PEG. Biomaterials, 23(13): 2641-2648. https://doi.org/10.1016/S0142-9612(01)00403-3
[10] Gupta, B., Agarwal, R., Sarwar Alam, M. (2013). Preparation and characterization of polyvinyl alcohol-polyethylene oxide-carboxymethyl cellulose blend membranes. Journal of Applied Polymer Science, 127(2): 1301-1308. https://doi.org/10.1002/app.37665
[11] Franco, P., De Marco, I. (2020). The use of poly(N-vinyl pyrrolidone) in the delivery of drugs: A review. Polymers, 12(5): 1114. https://doi.org/10.3390/polym12051114
[12] Teodorescu, M., Bercea, M. (2015). Poly(vinylpyrrolidone)-A versatile polymer for biomedical and beyond medical applications. Polymer-Plastics Technology and Engineering, 54(9): 923-943. https://doi.org/10.1080/03602559.2014.979506
[13] Feldstein, M.M., Shandryuk, G.A., Platé, N.A. (2001). Relation of glass transition temperature to the hydrogen-bonding degree and energy in poly(N-vinyl pyrrolidone) blends with hydroxyl-containing plasticizers. Part 1. Effects of hydroxyl group number in plasticizer molecule. Polymer, 42(3): 971-979. https://doi.org/10.1016/S0032-3861(00)00445-6
[14] Feldstein, M.M., Lebedeva, T.L., Shandryuk, G.A., et al. (1999). Complex formation in poly(vinylpyrrolidone)-poly(ethylene glycol) blends. Polymer Science Series A, 41(8): 867-875.
[15] Feldstein, M.M., Lebedeva, T.L., Shandryuk, G.A., Igonin, V.E., Avdeev, N.N., Kulichikhin, V.G. (1999). Stoichiometry of poly(N-vinylpyrrolidone)-poly(ethylene glycol) complex. Polymer Science Series A, 41: 867-875.
[16] Pires, P.C., Damiri, F., Zare, E.N., et al. (2024). A review on natural biopolymers in external drug delivery systems for wound healing and atopic dermatitis. International Journal of Biological Macromolecules, 263: 130296. https://doi.org/10.1016/j.ijbiomac.2024.130296
[17] Jin, S.G. (2026). Recent applications of chitosan-based biomaterials as wound dressings. International Journal of Molecular Sciences, 27(4): 1637. https://doi.org/10.3390/ijms27041637
[18] Anjum, S., Arora, A., Alam, M.S., Gupta, B. (2016). Development of antimicrobial and scar preventive chitosan hydrogel wound dressings. International Journal of Pharmaceutics, 508(1-2): 92-101. https://doi.org/10.1016/j.ijpharm.2016.05.013
[19] Mazhar, D., Afzal, S., Hassan, S., Imran, Z., Mehreen, S. (2026). Stimuli-responsive crosslinked chitosan/PVP/PEG hydrogel networks for targeted drug delivery and antimicrobial performance. Analytical Science Advances, 7(1): e70065. https://doi.org/10.1002/ansa.70065
[20] Rasool, A., Ata, S., Islam, A. (2019). Stimuli responsive biopolymer (chitosan) based blend hydrogels for wound healing application. Carbohydrate Polymers, 203: 423-429. https://doi.org/10.1016/j.carbpol.2018.09.083
[21] Sokker, H.H., Abdel Ghaffar, A.M., Gad, Y.H., Aly, A.S. (2009). Synthesis and characterization of hydrogels based on grafted chitosan for the controlled drug release. Carbohydrate Polymers, 75(2): 222-229. https://doi.org/10.1016/j.carbpol.2008.06.015
[22] Azeez, S., Sathiyaseelan, A., Venkatesan, K., Wang, M.H. (2024). Fabrication of mupirocin-loaded PEGylated chitosan nanoparticulate films for enhanced wound healing. International Journal of Molecular Sciences, 25(17): 9188. https://doi.org/10.3390/ijms25179188
[23] Aguilar-Ruiz, A.L., Madera-Santana, T.J., Sánchez-Duarte, R.G., Villegas-Peralta, Y., Aguilar-Ruiz, A.A., Orozco-Carmona, V.M. (2026). Development of chitosan polymer membranes with potential use in filtration processes. Membranes, 16(1): 31. https://doi.org/10.3390/membranes16010031
[24] Pereira, I.C., Duarte, A.S., Neto, A.S., Ferreira, J.M.F. (2019). Chitosan and polyethylene glycol based membranes with antibacterial properties for tissue regeneration. Materials Science and Engineering: C, 96: 606-615. https://doi.org/10.1016/j.msec.2018.11.029
[25] Rakkapao, N., Vao-soongnern, V., Masubuchi, Y., Watanabe, H. (2011). Miscibility of chitosan/poly(ethylene oxide) blends and effect of doping alkali and alkali earth metal ions on chitosan/PEO interaction. Polymer, 52(12): 2618-2627. https://doi.org/10.1016/j.polymer.2011.03.044
[26] Wardhono, E.Y., Pinem, M.P., Susilo, S., et al. (2022). Modification of physio-mechanical properties of chitosan-based films via physical treatment approach. Polymers, 14(23): 5216. https://doi.org/10.3390/polym14235216
[27] Patel, R.P., Patel, D.J., Bhimani, D.B., Patel, J.K. (2008). Physicochemical characterization and dissolution study of solid dispersions of furosemide with polyethylene glycol 6000 and polyvinylpyrrolidone K30. Dissolution Technologies, 15(3): 17-25. https://doi.org/10.14227/DT150308P17
[28] Feldstein, M.M., Kuptsov, S.A., Shandryuk, G.A., Platé, N.A., Chalykh, A.E. (2000). Coherence of thermal transitions in poly(N-vinyl pyrrolidone)-poly(ethylene glycol) compatible blends 3. Impact of sorbed water upon phase behaviour. Polymer, 41(14): 5349-5359.

https://doi.org/10.1016/S0032-3861(99)00681-3
[29] He, L.H., Xue, R., Yang, D.B., Liu, Y., Song, R. (2009). Effects of blending chitosan with PEG on surface morphology, crystallization and thermal properties. Chinese Journal of Polymer Science, 27(04): 501. https://doi.org/10.1142/S0256767909004175
[30] Chen, Y., Etxabide, A., Seyfoddin, A., Ramezani, M. (2023). Fabrication and characterisation of poly(vinyl alcohol)/chitosan scaffolds for tissue engineering applications. Materials Today: Proceedings. https://doi.org/10.1016/j.matpr.2023.02.303
[31] Çaykara, T., Alaslan, A., Eroğlu, M.S., Güven, O. (2006). Surface energetics of poly(N-vinyl-2-pyrrolidone)/chitosan blend films. Applied Surface Science, 252(20): 7430-7435. https://doi.org/10.1016/j.apsusc.2005.08.092
[32] Sethi, A.A., Mirza, E.H., Jawed, S.F. (2026). Development of chitosan: PVA/PEG polymer blends for skin graft applications. Advances in Polymer Technology, 18. https://doi.org/10.1155/adv/6644870
[33] Risbud, M.V., Bhat, S.V. (2001). Properties of polyvinyl pyrrolidone/β-chitosan hydrogel membranes and their biocompatibility evaluation by haemorheological method. Journal of Materials Science: Materials in Medicine, 12(1): 75-79. https://doi.org/10.1023/A:1026769422026
[34] Hanhijärvi, K., Majava, T., Kassamakov, I. (2010). Scratch resistance of plasticized hydroxypropyl methylcellulose (HPMC) films intended for tablet coatings. European Journal of Pharmaceutics and Biopharmaceutics, 74(2): 371-376. https://doi.org/10.1016/j.ejpb.2009.09.006